inorganics

MDPI

Article

Fluoro-Germanium (IV) Cations with Neutral Co-Ligands—Synthesis, Properties and Comparison with Neutral GeF_4 Adducts

Madeleine S. Woodward [1], Rhys P. King [1], Robert D. Bannister [1], Julian Grigg [2], Graeme McRobbie [2], William Levason [1] and Gillian Reid [1,*]

[1] School of Chemistry, University of Southampton, Southampton SO17 1BJ, UK; m.s.woodward@soton.ac.uk (M.S.W.); r.p.king@soton.ac.uk (R.P.K.); r.d.bannister@soton.ac.uk (R.D.B.); wxl@soton.ac.uk (W.L.)

[2] GE Healthcare, Pollards Wood, Nightingales Lane, Chalfont St Giles, Bucks HP8 4SP, UK; julian.grigg@ge.com (J.G.); graeme.mcrobbie@ge.com (G.M.)

* Correspondence: G.Reid@soton.ac.uk

Abstract: The reaction of $[GeF_4L_2]$, L = dmso (Me_2SO), dmf (Me_2NCHO), py (pyridine), pyNO (pyridine-N-oxide), $OPPh_3$, $OPMe_3$, with $Me_3SiO_3SCF_3$ (TMSOTf) and monodentate ligands, L, in a 1:1:1 molar ratio in anhydrous CH_2Cl_2 formed the monocations $[GeF_3L_3][OTf]$. These rare trifluoro-germanium (IV) cations were characterised by microanalysis, IR, ^1H, $^{19}F\{^1H\}$ and, where appropriate, $^{31}P\{^1H\}$ NMR spectroscopy. The $^{19}F\{^1H\}$ NMR data show that in CH_3NO_2 solution the complexes exist as a mixture of *mer* and *fac* isomers, with the *mer* isomer invariably having the higher abundance. The X-ray structure of *mer*-$[GeF_3(OPPh_3)_3][OTf]$ is also reported. The attempts to remove a second fluoride using a further equivalent of TMSOTf and L were mostly unsuccessful, although a mixture of $[GeF_2(OAsPh_3)_4][OTf]_2$ and $[GeF_3(OAsPh_3)_3][OTf]$ was obtained using excess TMSOTf and $OAsPh_3$. The reaction of $[GeF_4(MeCN)_2]$ with TMSOTf in CH_2Cl_2 solution, followed by the addition of 2,2′:6′,2″-terpyridine (terpy) formed *mer*-$[GeF_3(terpy)][OTf]$, whilst a similar reaction with 1,4,7-trimethyl-1,4,7-triazacyclononane (Me_3-tacn) in MeCN solution produced *fac*-$[GeF_3(Me_3\text{-tacn})][OTf]$. Dicationic complexes bearing the GeF_2^{2+} fragment were isolated using the tetra-aza macrocycles, 1,4,7,10-tetramethyl-1,4,7,10-tetra-azacyclododecane (Me_4-cyclen) and 1,4,8,11-tetramethyl-1,4,8,11-tetra-azacyclotetradecane (Me_4-cyclam), which reacted with $[GeF_4(MeCN)_2]$ and two equivalents of TMSOTf to cleanly form the dicationic difluoride salts, *cis*-$[GeF_2(Me_4\text{-cyclen})][OTf]_2$ and *trans*-$[GeF_2(Me_4\text{-cyclam})][OTf]_2$. The $^{19}F\{^1H\}$ NMR spectroscopy shows that in CH_3NO_2 solution there are four stereoisomers present for *trans*-$[GeF_2(Me_4\text{-cyclam})][OTf]_2$, whereas the smaller ring-size of Me_4-cyclen accounts for the formation of only *cis*-$[GeF_2(Me_4\text{-cyclen})][OTf]$, and is confirmed crystallographically. New spectroscopic data are also reported for $[GeF_4(L)_2]$ (L = dmso, dmf and pyNO). Density functional theory calculations were used to probe the effect on the bonding as fluoride ligands were sequentially removed from the germanium centre in the $OPMe_3$ complexes.

Keywords: germanium; fluoride; cations; crystal structures

Citation: Woodward, M.S.; King, R.P.; Bannister, R.D.; Grigg, J.; McRobbie, G.; Levason, W.; Reid, G. Fluoro-Germanium (IV) Cations with Neutral Co-Ligands—Synthesis, Properties and Comparison with Neutral GeF_4 Adducts. *Inorganics* **2022**, *10*, 107. https://doi.org/10.3390/inorganics10080107

Academic Editors: Stephen Mansell, Simon Aldridge and Cameron Jones

Received: 21 June 2022
Accepted: 13 July 2022
Published: 27 July 2022

1. Introduction

Transition-metal halides, especially those from the 3*d* series, are very frequently used as the metal source for the introduction of the transition-metal ion to a wide range of ligand types, from monodentates to chelates, to form coordination complexes, with easy and often spontaneous displacement of the halides [1]. In contrast, the *p*-block halides often retain the halides, and formation of cationic species with *p*-block Lewis acids derived from *p*-block halides is much less common.

The coordination chemistry of *p*-block elements containing the heavier halide co-ligands (Cl, Br or I) has been studied in great detail for over 50 years [1–5]. In marked

contrast, after some preliminary study, that of the corresponding fluorides (except BF_3), was neglected until recent years [6]. In part, this reflected the limited commercial availability of the fluorides, which even when available, were often of unknown and doubtful purity. Additionally, studies were hindered by the fact that the fluorides of the more metallic elements were strongly polymerised, inert solids, which rarely offered facile routes to their complexes [6,7]. In some cases within Group 13, only the more reactive hydrated MF_3 precursors could be used, and even then they sometimes required hydrothermal conditions [6–9].

Recent studies of the coordination chemistry of *p*-block fluorides have been driven by the recognition that the complexes of the fluorides often have very different properties than those containing the heavier halides [6,7], and also in part by the search for new carriers of the radioisotope $[^{18}F]F^-$, which is widely used in medical diagnostics for PET (positron emission tomography) imaging [7,10,11]. In this regard, the *p*-block systems have attracted interest due to their high M-F bond dissociation energies, and their ability to incorporate $[^{18}F]F^-$ under mild conditions (e.g., aqueous solution, near room temperature and close to neutral pH) and in the final step of the process.

Within Group 14, the development of soluble synthons such as $[SnF_4(MeCN)_2]$ [12] or $[GeF_4(MeCN)_2]$ [13], from which the weakly bound MeCN could be readily displaced by other neutral ligands, was a major advance. The $[GeF_4(MeCN)_2]$ is both easier to handle and to control the stoichiometry, compared to using GeF_4, which is a gas at ambient temperatures (Sub. 236 K) [13]. As a result of these more recent studies, a range of neutral ligand complexes of GeF_4 with N- or O-donor ligands has been thoroughly characterised, e.g., $[GeF_4L_2]$ (L = OPR_3, $OAsR_3$, py) and $[GeF_4(L\text{-}L)]$ (L-L = $R_2P(O)(CH_2)_nP(O)R_2$, bipy (2,2′-bipyridyl), phen (1,10-phenanthroline), $Me_2N(CH_2)_2NMe_2$). The crystal structures of representative examples have also been reported [13,14].

Examples of soft donor ligand complexes, such as with tertiary phosphines, include *trans*-$[GeF_4(PR_3)_2]$ (R = Me, Ph, ^{i}Pr), *cis*-$[GeF_4\{R_2P(CH_2)_2PR_2\}]$ (R = Me, Et, Ph, Cy), and *cis*-$[GeF_4\{o\text{-}C_6H_4(PR_2)_2\}]$ (R = Me, Ph) [15,16], while dithioether ligands yield species such as *cis*-$[GeF_4\{RS(CH_2)_2SR\}]$ (R = Me, Et) [17], which have also been thoroughly characterised. Notably, the tri- and tetra-phosphines, $MeC(CH_2PPh_2)_3$ and $P(CH_2CH_2PPh_2)_3$ (L) form complexes of the type $[GeF_4(L)]$, with the polyphosphine κ^2-coordinated, and the free arms are unable to displace fluoride from the germanium [16]. Uniquely, the triaza macrocycle, Me_3-tacn (Me_3-tacn = 1,4,7-trimethyl-1,4,7-triazacyclononane) reacts with $[GeF_4(MeCN)_2]$ in CH_2Cl_2 solution to form a cation in the $[GeF_3(Me_3\text{-tacn})]_2[GeF_6]$ salt [14]. The X-ray crystal structure of $[GeF_3(Me_3\text{-tacn})]Cl$ confirms the presence of a *fac*-octahedral GeF_3N_3 unit in the cation. In contrast, the tetra-aza macrocycle Me_4-cyclam (1,4,8,11-tetramethyl-1,4,8,11-tetra-azacyclotetradecane) forms the neutral $[GeF_4(\kappa^2\text{-}Me_4\text{-cyclam})]$ or $[(GeF_4)_2(\mu\text{-}\kappa^2\kappa'^2\text{-}Me_4\text{-cyclam})]$, in which the macrocycle is bound *exodentate* to the GeF_4 units [14].

A new route to cationic germanium (IV) fluoride complexes via the oxidation of germanium (II) adducts has also been reported. The tetradentate N-donor ligand, *tris*(1-ethylbenzoimidazol-2-ylmethyl)amine ($BIMEt_3$) forms the Ge (II) complex, $[Ge(BIMEt_3)][OTf]_2$, which, upon treatment with XeF_2 or *Selectfluor*, produces $[GeF_2(BIMEt_3)][OTf]_2$ [18]. The X-ray structure of this species reveals a distorted octahedron with *cis* fluorines. The treatment of $[GeF_2(BIMEt_3)][OTf]_2$ with TMSOTf (TMSOTf = $Me_3SiO_3SCF_3$) generates $[GeF(BIMEt_3)OTf][OTf]_2$, in which a coordinated triflate completes the six-coordination at germanium.

Since cationic fluoro-germanium (IV) complexes with most neutral ligands do not form directly from GeF_4, we explored the use of halide abstraction reagents. This approach is exemplified by using $AlCl_3$ to remove chloride from various tin (IV) phosphine complexes, forming cationic $[SnCl_3(PR_3)_2][AlCl_4]$, $[SnCl_2(PR_3)_2][AlCl_4]_2$ (R = Me, Et), $[SnCl_3\{o\text{-}C_6H_4(PMe_2)_2\}][AlCl_4]$ and $[SnCl_2\{o\text{-}C_6H_4(PMe_2)_2\}][AlCl_4]_2$ [19,20]. A similar reaction using $Na[BAr^F]$ (BAr^F = B{3,5-$CF_3(C_6H_3)_4$}) and the corresponding neutral tetrahalide complex produced the five-coordinate species $[SnCl_3(PEt_3)_2][BAr^F]$ and $[SnCl_3(AsEt_3)_2][BAr^F]$ [20].

In the corresponding tin fluoride systems, AlF_3 did not behave as a fluoride abstractor as it is an inert polymer [6], while reactions with $Na[BAr^F]$ did not go to completion [21]. Therefore, we explored using TMSOTf. This has previously proved to be an efficient halide abstractor in group 14 halide chemistry, predominantly with the group 14 tetrachlorides [20,22], and in tin (IV) and germanium (IV) fluoride phosphine systems [16,21]. In the majority of the phosphine cases, the halide abstraction resulted in complexes with weakly coordinated triflate, rather than salts containing genuine cationic species. Examples included $[SnF_{4-n}(PMe_3)_2(OTf)_n]$ (n = 1–3) [21], $[GeF_{4-n}(PMe_3)_2(OTf)_n]$ (n = 1–3), and $GeF_{4-n}\{o\text{-}C_6H_4(PMe_2)_2\}(OTf)_n]$ (n = 1–3) [16]. In the case of Sn (IV), the reactions of $[SnF_4L_2]$ (L = dmso, py, pyNO, dmf, $OPPh_3$) with one equivalent each of TMSOTf and L produced $[SnF_3L_3]$OTf cations, shown by NMR studies to be a mixture of *mer* and *fac* isomers in solution [21]. The attempts to remove a further fluoride using a second equivalent of TMSOTf and more L in most cases resulted in a mixture of $[SnF_3L_3]$OTf and $[SnF_2L_4][OTf]_2$, although $[SnF_2(OPPh_3)_4][OTf]_2$ was isolated and shown by an X-ray structure to be the *trans* isomer in the solid state. The NMR studies showed a mixture of the *cis* and *trans* form of this dication present in solution [21].

Here we report attempts to isolate fluoro-germanium (IV) cations with a range of neutral N- and O-donor ligands, including the N_3- and N_4-donor macrocyclic ligands. A comparison of the key spectroscopic data for $[GeF_4L_2]$ and $[GeF_3L_3]^+$ types with the tin analogues and an exploration of the bonding via DFT calculations are reported, together with the promotion of *endocyclic* coordination of the tetra-aza macrocycles, yielding germanium difluoride dications.

2. Results

$[GeF_4L_2]$: $[GeF_4L_2]$ (L = dmso, dmf, py, pyNO, $OPPh_3$, $OPMe_3$, $OAsPh_3$) were prepared by the direct reaction of $[GeF_4(MeCN)_2]$ with the ligands. The complexes with py, $OPPh_3$, $OPMe_3$, $OAsPh_3$ have been previously described [13,14] and the characterisation data in the present study were consistent with the published data. The X-ray crystal structures of *trans*-$[GeF_4L_2]$ (L = py, $OPPh_3$, $OPMe_3$) and *cis*-$[GeF_4(FCH_2CN)_2]$ have also been previously reported [13,14,23]. Their ^{19}F NMR spectroscopic data are given in Table 1.

Table 1. Selected NMR spectroscopic data.

Complex	Solvent Temperature	$^{19}F\{^1H\}$ NMR/ppm [a]	$^2J_{FF}$/Hz	$^{31}P\{^1H\}$ NMR/ppm	Reference
$[GeF_4(dmso)_2]$ *cis* *trans*	CD_3NO_2 253 K	−115.3 (t), −129.8 (t) −115.4 (s)	61		This work
$[GeF_3(dmso)_3][OTf]$ *mer* *fac*	CD_3NO_2 253 K	−109.8 (d), −121.7 (t) −122.2 (s)	71		This work
$[GeF_4(dmf)_2]$ *cis* *trans*	CD_3NO_2 253 K	−125.4 (t), −135.8 (t) −125.4 (s)	59		This work
$[GeF_3(dmf)_3][OTf]$ *mer* *fac*	CD_3NO_2 253 K	−126.1 (d) −135.0 (t) −134.5 (s)	64		This work
$[GeF_4(py)_2]$ *trans*	$CDCl_3$ 253 K	−125.7 (s)			Ref. [14]
$[GeF_3(py)_3][OTf]$ *mer* *fac*	CD_2Cl_2 298 K	−122.0 (d), −137.3 (t) −149.2 (s)	55		This work

Table 1. *Cont.*

Complex	Solvent Temperature	$^{19}F\{^1H\}$ NMR/ppm [a]	$^2J_{FF}$/Hz	$^{31}P\{^1H\}$ NMR/ppm	Reference
$[GeF_4(pyNO)_2]$ *cis* *trans*	CD_3NO_2 298 K 253 K	−142.8 (br s) −136.1 (t), −133.1 (t) −129.8 (s)	58		This work
$[GeF_3(pyNO)_3][OTf]$ *mer* *fac*	CD_3NO_2 253 K	−136.8 (d), −143.0 (t) −141.8 (s)	65		This work
$[GeF_4(OPPh_3)_2]$ *cis* *trans*	$CDCl_3$ 253 K	−100.9 (t), −120.6 (t) −105.3 (s)	64	40.8 (s) 40.2 (s)	Ref. [13]
$[GeF_3(OPPh_3)_3][OTf]$ *mer* *fac*	CD_2Cl_2 298 K	−89.0(d), −100.4(t) −100.9(s)	76	44.1 (s) 41.7 (s) 43.7 (s)	This work
$[GeF_4(OPMe_3)_2]$ *cis* *trans*	CD_2Cl_2 298 K	−107.6 (t), −121.6 (t) −109.9 (s)	58	65.1 (s) 65.8 (s)	Ref. [13]
$[GeF_3(OPMe_3)_3][OTf]$ *mer* *fac*	CD_3NO_2 298 K	−95.6 (d), −106.6 (t) −93.0 (s)	64	67.4 (m), 66.9 (m) 70.4 (s)	This work
$[GeF_4(OAsPh_3)_2]$ *cis* *trans*	CD_2Cl_2 298 K	−94.4 (t), −112.9 (t) −98.2 (s)	60		Ref. [13]
$[GeF_3(OAsPh_3)_3]OTf$ [b] *mer* *fac*	CD_3NO_2 298K	−79.3 (d), −89.5 (t) −89.9 (s)	68		This work
$[GeF_2(OAsPh_3)_4][OTf]_2$ [b] *cis* *trans*	CD_3NO_2 298K	−65.1 (s) −59.1 (s)			This work
$[GeF_4(MeCN)_2]$ *cis* *trans*	CD_2Cl_2 180 K	−101.2 (t), −134.2 (t) −108.2 (s)	55		Ref. [13]
fac-$[GeF_3(Me_3\text{-tacn})][OTf]$	CD_3NO_2 298 K	−151.7 (s)			This work
mer-$[GeF_3(terpy)][OTf]$	CD_2Cl_2 298 K	−115.9 (d), −153.0 (t)	68		This work
$[GeF_2(Me_4\text{-cyclen})][OTf]_2$ *cis*	CD_3NO_2 298 K	−132.3 (s)			This work
$[GeF_2(Me_4\text{-cyclam})][OTf]_2$ *trans*	CD_3NO_2 298 K	−136.8 (d) −134.8 (d) −132.7 (s) −132.2 (d) −130.8 (d) −130.5 (s)	38 52 38 52		This work

[a] triflate resonances omitted; [b] not isolated in a pure state, data from a mixture with $[GeF_2(OAsPh_3)_4][OTf]_2$ and $[GeF_3(OAsPh_3)_3][OTf]$.

In solution at low temperatures, the $^{19}F\{^1H\}$ NMR data typically show two 1:1 triplets and a singlet indicating the presence of both *cis* and *trans* isomers (Figure 1) [13,14], although the ambient temperature spectra of some are consistent with exchanging systems, (Table 1) and the relative amounts of the isomers vary with the solvent. Full details of the spectra of the new complexes are given in the Experimental section and the SI. The $^{19}F\{^1H\}$ NMR spectra of $[GeF_4(dmso)_2]$ and $[GeF_4(dmf)_2]$ in CH_3NO_2 show one sharp singlet and two

broad lines at 298 K; on cooling to 253 K, the broad lines resolve into the expected triplets (Figures S1.4 and S2.4). This suggests that dissociative neutral ligand exchange is easier in the *cis* isomers, whilst the *trans* isomers are not involved.

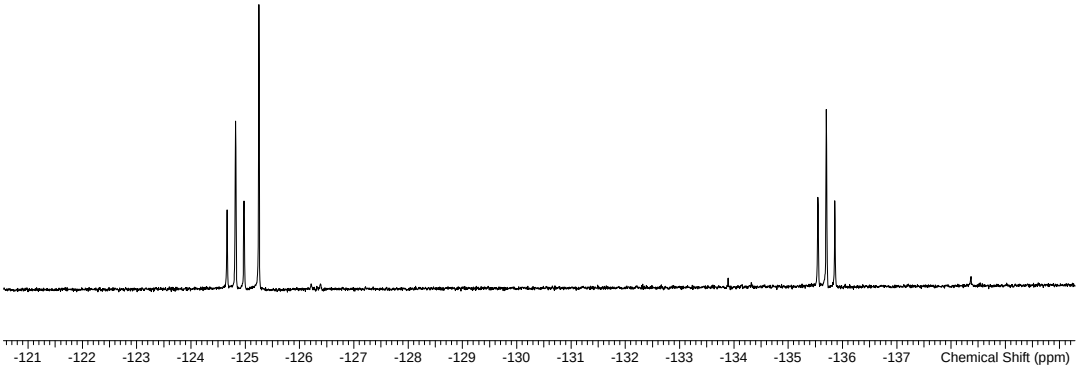

Figure 1. The $^{19}F\{^{1}H\}$ NMR spectrum of the *cis/trans*-isomer mixture from $[GeF_4(dmf)_2]$ in CH_3NO_2 at 253 K.

$[GeF_3L_3][OTf]$: The general approach to the synthesis of the trifluoro-germanium cations utilised the reaction of $[GeF_4L_2]$ with one equivalent of TMSOTf in anhydrous CH_2Cl_2, followed by the addition of a further equivalent of L (Scheme 1).

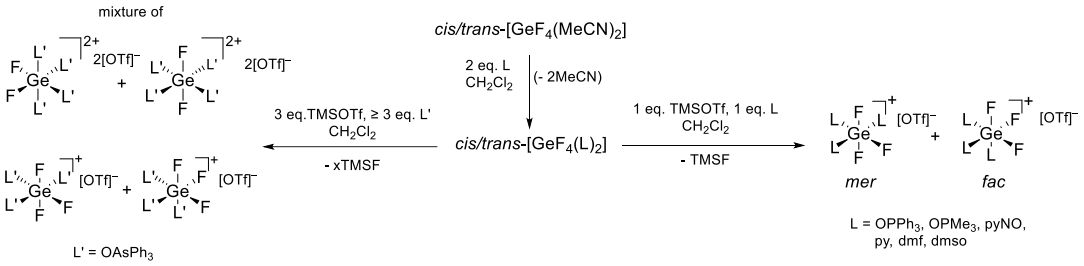

Scheme 1. Synthesis of the complexes produced in this work containing monodentate ligands L or L′.

The reaction of $[GeF_4(MeCN)_2]$ with TMSOTf in MeCN caused decomposition, but with the other ligands (L = dmso, dmf, py, pyNO, $OPPh_3$, $OPMe_3$) the products were $[GeF_3L_3]OTf$. Crystals of $[GeF_3(OPPh_3)_3][OTf]$ were obtained from CH_2Cl_2 solution by slow evaporation and the X-ray structure analysis revealed them to be the *mer* isomer (Figure 2).

The structure reveals a near regular octahedral geometry with the d(Ge-F) and d(Ge-O) showing no significant effect of the *trans* ligands. A comparison with the structure of *trans*-$[GeF_4(OPPh_3)_2]$ [13] shows that the d(Ge-F) are identical, but the d(Ge-O) is slightly longer in the latter.

The cations were generally poorly soluble in chlorocarbons, and data were mostly obtained from the CH_3NO_2/CD_3NO_2 solutions, which have the limitation of a high M.P. (245 K), hence precluding lower temperature studies, but stronger donor solvents were avoided since they tend to displace the neutral ligands. The $^{19}F\{^{1}H\}$ NMR spectra show the presence of both *mer* and *fac* isomers with the former producing a doublet [2F] and a triplet [F] and the latter a singlet; usually the *mer* isomer is the more abundant. Figure 3 shows a typical example. The $^{19}F\{^{1}H\}$ NMR resonances (Table 1) occur in the range of $\delta = -80$ to -155 depending upon the isomer and the neutral ligand present, and overlap with those of $[GeF_4L_2]$, although the δ(F) *trans* F are always at a higher frequency than the δ(F) *trans* N/O for a particular complex.

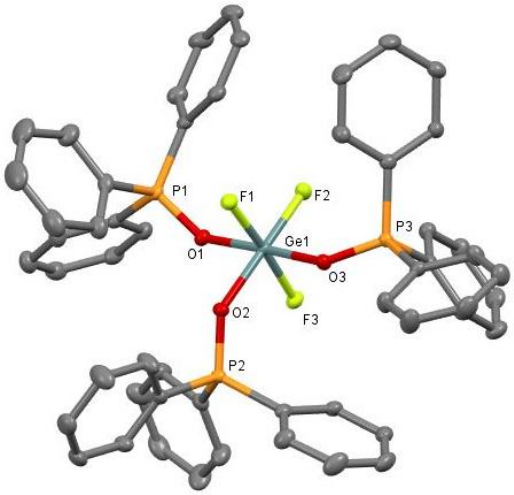

Figure 2. View of the molecular structure of the cation in *mer*-$[GeF_3(OPPh_3)_3][OTf]$ showing the atom numbering scheme. A second similar, but crystallographically independent, molecule of *mer*-$[GeF_3(OPPh_3)_3][Otf]$ in the asymmetric unit, and the H atoms are omitted for clarity. Ellipsoids are drawn at the 50% probability level. Selected bond lengths (Å) and angles (°): Ge1-F3 = 1.7598 (11), Ge1-F1 = 1.7679 (11), Ge1-F2 = 1.7628 (11), Ge1-O2 = 1.8950 (13), Ge1-O3 = 1.9076 (13), Ge1-O1 = 1.8990 (13), P3-O3 = 1.5287 (14), P2-O2 = 1.5298 (13), P1-O1 = 1.5232 (13), F3-Ge1-F2 = 91.99 (5), F2-Ge1-F1 92.69 (5), O2-Ge1-O3 = 88.38 (6), O2-Ge1-O1 = 89.30 (6).

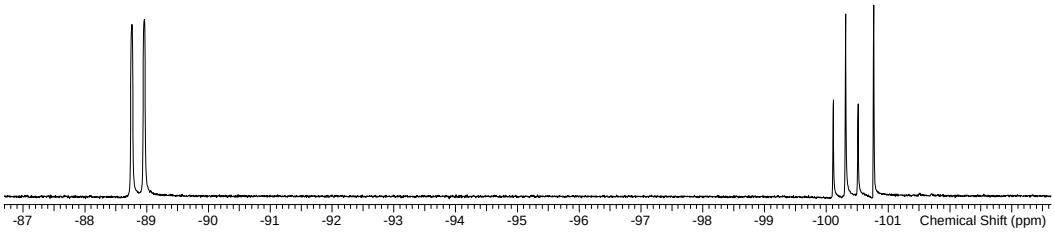

Figure 3. The $^{19}F\{^1H\}$ NMR spectrum of the *mer/fac*-isomer mixture in $[GeF_3(OPPh_3)_3][Otf]$ (CD_2Cl_2, 298 K); the Otf resonance is omitted for clarity.

$[GeF_3(pyNO)_3][Otf]$ appears to be somewhat unstable in CD_3NO_2 solution, decomposing slowly at room temperature over the period of the NMR acquisition, and the $^{19}F\{^1H\}$ NMR spectra usually show some $[GeF_4(pyNO)_2]$ present (SI Figure S7.2). The $[GeF_3(OPR_3)_3][Otf]$ (R = Me, Ph) complexes were obtained in good yield and were stable in CD_3NO_2 solution; the *mer* isomer is the major form in both (Figure 3). In addition to the $^2J_{FF}$ coupling, the $^{19}F\{^1H\}$ and $^{31}P\{^1H\}$ NMR spectra of $[GeF_3(OPMe_3)_3][Otf]$ (Figure S9) show further small couplings of ~ 7 Hz which were tentatively assigned as $^3J_{FP}$. Similar couplings are evident, but less well resolved, in the spectra of $[GeF_3(OPPh_3)_3][Otf]$.

In marked contrast, the reaction of $[GeF_4(MeCN)_2]$, TMSOTf and $OasPh_3$ in a 1:1:3 molar ratio in CH_2Cl_2 precipitated a white solid. The $^{19}F\{^1H\}$ NMR spectrum (in CD_3NO_2) shows the expected resonances for $[GeF_3(OasPh_3)_3][Otf]$, *viz*, δ = −89.9 (s), *fac* isomer; −89.5 (t, $^2J_{FF}$ = 66 Hz), −79.3 ($^2J_{FF}$ = 67 Hz), *mer* isomer, and −79.9 (s, Otf), along with two strong singlets at δ = −65.1 and −59.1. By comparison with the spectra of $[GeF_2$(tetraazamacrocycle)$][Otf]_2$ (*vide infra*), these were assigned to *cis*- and *trans*-$[GeF_2(OasPh_3)_4][Otf]_2$ (Figure 4). Integration of the $^{19}F\{^1H\}$ NMR spectrum of the mixture suggested that the ratio of the complexes $[GeF_3(OasPh_3)_3][Otf]$: $[GeF_2(OasPh_3)_4][Otf]_2$ was ~3:1. Attempts to obtain a pure sample of either were unsuccessful, although their identities are not in doubt.

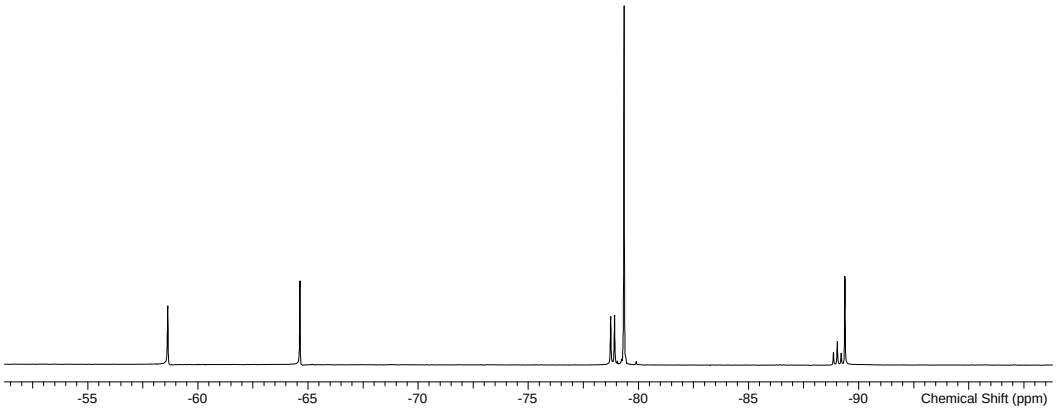

Figure 4. $^{19}F\{^{1}H\}$ NMR spectrum (CD_3NO_2, 298 K) from a mixture of $[GeF_3(OasPh_3)_3][Otf]$ and $[GeF_2(OasPh_3)_4][Otf]_2$.

The ability of $OasPh_3$ to form $[GeF_2(OasPh_3)_4][Otf]_2$ contrasts with the other ligands (including OPR_3, R = Me or Ph) and would indicate that the arsine oxide is a stronger donor towards the fluoro-germanium (IV) centre. A comparison of X-ray crystallographic data on several isostructural transition-metal pnictine oxide complexes showed that M-Oas was shorter than M-OP, which is evidence for the stronger binding of the $OasPh_3$ towards hard acceptors [24–26].

$[GeF_3(L')][OTf]$ (L′ = Me_3-tacn, terpy): As indicated in the Introduction, the triaza macrocycle Me_3-tacn was the only ligand able to directly form a cation upon reaction with GeF_4 in anhydrous CH_2Cl_2, in the "self ionisation" complex $[GeF_3(Me_3\text{-tacn})]_2[GeF_6]$ [14]. This complex was insoluble in common solvents, but a crystal fortuitously obtained from the solid after extraction with CH_2Cl_2 was shown by X-ray structure determination to be $[GeF_3(Me_3\text{-tacn})]Cl$, which is the chloride arising from the attack on the solvent by the displaced fluoride ion. The reaction of $[GeF_4(MeCN)_2]$ with TMSOTf in anhydrous MeCN, followed by the addition of Me_3-tacn formed *fac*-$[GeF_3(Me_3\text{-tacn})]OTf$ (Scheme 2), which was much more soluble and allowed the solution NMR data for the cation to be obtained. The $^{19}F\{^{1}H\}$ spectrum, which shows a singlet at −151.7 ppm, is consistent with the expected *fac* geometry. In the earlier study [14], the direct reaction of GeF_4 with terpy in CH_2Cl_2 yielded an insoluble product of the composition $[(GeF_4)_3(terpy)_2]$, and since the IR spectrum of this complex did not show features characteristic of $[GeF_6]^{2-}$ [27], it was suggested to be oligomeric with both bridging and chelating terpy ligands. Here we found that the sequential reaction of $[GeF_4(MeCN)_2]$ with TMSOTf and terpy (terpy = terpyridine) in CH_2Cl_2 solution (Scheme 2), afforded white $[GeF_3(terpy)]OTf$, whose $^{19}F\{^{1}H\}$ NMR spectrum contains (in addition to the OTf resonance) resonances at −115.9 (d, [2F], $^{2}J_{FF}$ = 68 Hz) and −153.0 (t, [F], $^{2}J_{FF}$ = 68 Hz), showing the presence of the expected *mer* cation. However, the product did not fully dissolve for the NMR spectra (see Materials and Methods section).

$[GeF_2(L'')][OTf]_2$ (L″ = Me_4-cyclen or Me_4-cyclam): The direct reaction of $[GeF_4(MeCN)_2]$ with Me_4-cyclam in CH_2Cl_2 precipitated a white powder, identified as $[(GeF_4)_2(\mu\text{-}Me_4\text{-cyclam})]$, whilst a few crystals grown from the filtrate proved to be $[GeF_4(\kappa^2\text{-}Me_4\text{-cyclam})]$ [14]. In contrast, the reaction of $[GeF_4(MeCN)_2]$ with two molar equivalents of TMSOTf in MeCN, followed by addition of Me_4-cyclen or Me_4-cyclam afforded the dications $[GeF_2(L'')][OTf]_2$ in good yields (Scheme 3). For $[GeF_2(Me_4\text{-cyclen})][OTf]_2$ the ^{1}H NMR spectrum exhibits two Me resonances of equal intensity and a singlet resonance in the $^{19}F\{^{1}H\}$ NMR spectrum, indicating that the 12-membered ring generated the *cis*-octahedral isomer. This was confirmed by an X-ray crystal structure analysis of $[GeF_2(Me_4\text{-cyclen})][OTf]_2{\cdot}xCH_3NO_2$ (see Materials and Methods section for discussion of this inversion twin) (Figure 5).

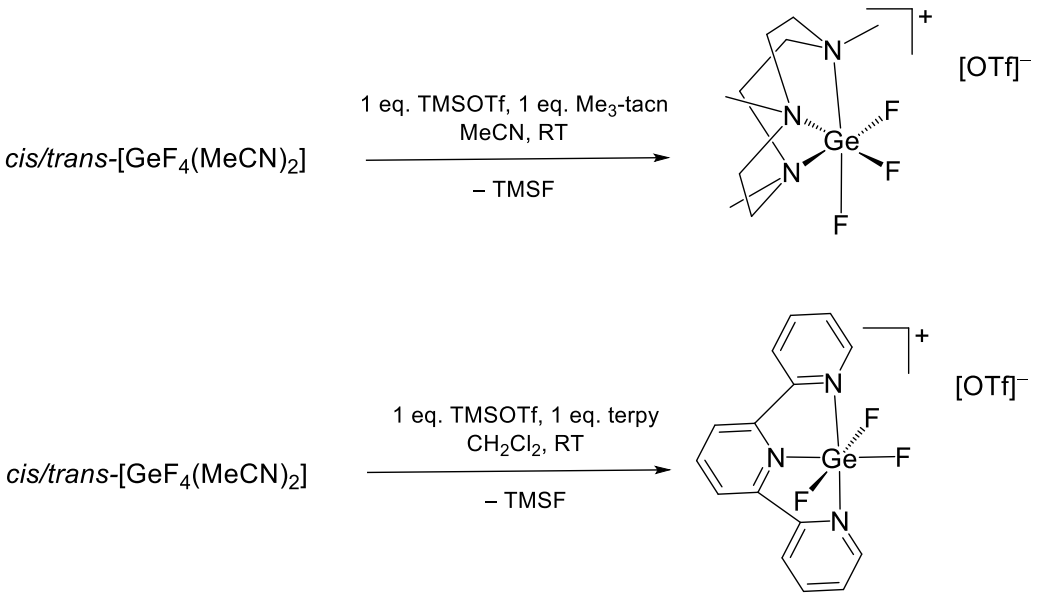

Scheme 2. Routes used to prepare complexes with the tridentate Me_3-tacn and terpy ligands.

In contrast, the corresponding spectra of $[GeF_2(Me_4\text{-cyclam})][OTf]_2$ exhibit six $^{19}F\{^1H\}$ resonances (Figure 6), four doublets and two singlets. These may be attributed to the presence of four of the five possible stereoisomers (with the Me groups '*all up*', '*up,up,up,down*', '*up,up,down,down*'—2 variants and '*up,down,up,down*' relative to the GeN_4 plane) of a *trans* octahedral geometry with slow pyramidal inversion at N; the larger (14-membered) ring of Me_4-cyclam allowing the germanium to sit within the ring. The coordinated fluorides are inequivalent in the '*all up*' and '*up,up,up,down*' forms, accounting for the four doublets, whilst the two singlets probably correspond to the equivalent fluorines in the other two stereoisomers. We cannot rule out the possibility that one of the singlets corresponds to a *cis* isomer, but this seems less likely.

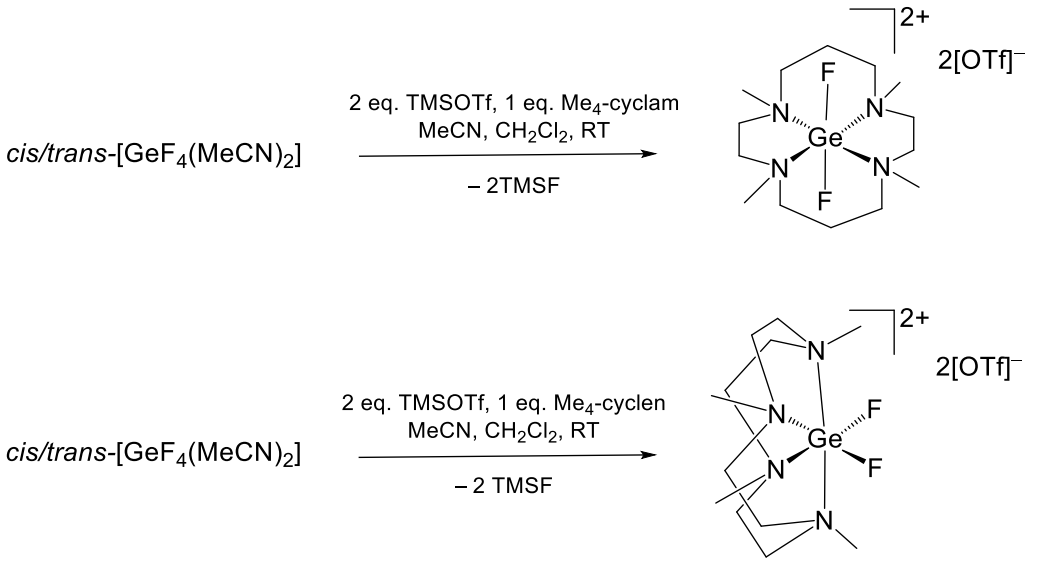

Scheme 3. Synthesis of the tetra-aza macrocyclic complexes.

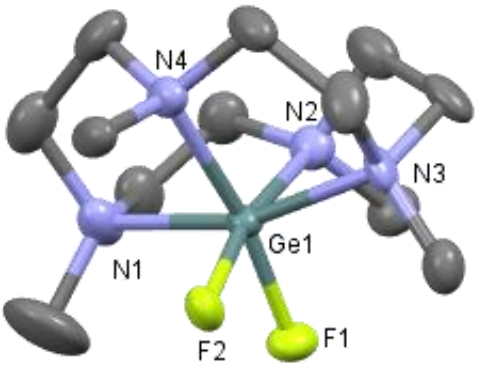

Figure 5. The molecular structure of one of the 14 crystallographically independent *cis*-$[GeF_2(Me_4\text{-cyclen})]^{2+}$ dications within the unit cell (see Experimental for details). Ellipsoids are drawn at the 50% probability level and H-atoms are omitted for clarity. Selected bond lengths (Å) and angles (°): Ge1-F1 = 1.755 (8), Ge1-F2 = 1.792 (8), Ge1-N1 = 2.101 (12), Ge1-N2 = 2.084 (11), Ge1-N3 = 2.035 (11), Ge1-N4 = 2.107 (11), F1-Ge1-F2 = 84.5 (4), N1-Ge1-N4 = 83.8 (5), N2-Ge1-N1 = 84.9 (5), N2-Ge1-N4 = 106.2 (4), N3-Ge1-N1 = 161.7 (5), N3-Ge1-N2 = 84.8 (5), N3-Ge1-N4 = 84.6 (5). The bond distances and angles in the other molecules are broadly similar, but the combination of the unexpectedly large unit cell and the inversion twin preclude detailed comparisons.

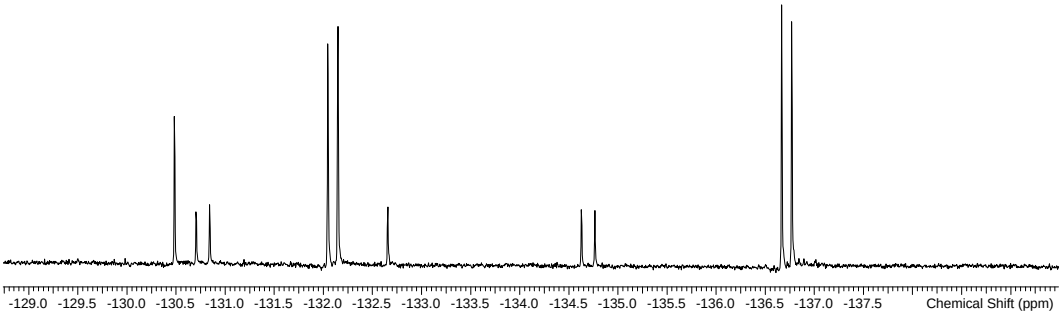

Figure 6. $^{19}F\{^1H\}$ NMR spectrum of $[GeF_2(Me_4\text{-cyclam})][OTf]_2$ showing four doublets and two singlets, corresponding to those of the four stereoisomers with Me groups '*all up*', 2× '*up,up,down,down*', and '*up,down,up,down*'. The OTf resonance is not shown.

DFT Calculations

The DFT calculations were performed on the neutral complexes *cis*/*trans*-$[GeF_4(OPMe_3)_2]$, the monocations, *mer*/*fac*-$[GeF_3(OPMe_3)_3]^+$, and the dications *cis*/*trans*-$[GeF_2(OPMe_3)_4]^{2+}$ using the B3LYP-D3 functional and 6-311G(d) basis set. For *trans*-$[GeF_4(OPMe_3)_2]$ the initial geometry was taken from the published crystal structure [13], whereas for the *cis* isomer the structure was constructed starting from the *trans* geometry. Both structures were optimised, and the calculations converged with no imaginary frequencies. For the monocationic *mer*/*fac*-$[GeF_3(OPMe_3)_3]^+$, the geometry of the *mer* isomer was taken from the structure of $[GeF_3(OPPh_3)_3]^+$ with the Ph groups modified to Me. For the *fac* isomer the converged structure of *mer*-$[GeF_3(OPMe_3)_3]^+$ was taken as a starting point. The dicationic complexes *trans*/*cis*-$[GeF_2(OPMe_3)_4]^{2+}$ were also modelled, with *trans*-$[SnF_2(OPPh_3)_4]^{2+}$ [21] taken as the starting geometry for the *trans* isomer. For the *cis* isomer the initial geometry was taken from the optimised geometry of *trans*-$[GeF_2(OPMe_3)_4]^{2+}$ and the structure was modified to yield the *cis* geometry.

Comparing the geometric isomers of $[GeF_4(OPMe_3)_2]$, the *cis* isomer is only very slightly lower in energy by 1.31 kJ/mol (compared to RT = 2.48 kJ/mol) in the gas phase (Table S2). This is consistent with the experimental observation that both isomers are seen in solution, although in this case the position of the equilibrium will be affected by the chosen solvent. For the trifluoro monocations, the *mer* isomer is slightly more stable than the *fac* by 3.19 kJ/mol, which is also consistent with the solution state data, which indicate that *mer*-$[GeF_3(OPMe_3)_3]^+$ is the more abundant isomer. For the dications *cis*/*trans*-

$[GeF_2(OPMe_3)_4]^{2+}$, the calculations show that the *cis* isomer is much more stable than the *trans* isomer (18.50 kJ/mol lower in energy) (although we were unable to isolate these dications). For both isomers of $[GeF_4(OPMe_3)_2]$ the HOMO, HOMO-1 and HOMO-2 are combinations of lone pairs based on the fluorine ligands and the oxygens of the $OPMe_3$ ligand (Figure S7). The LUMO and LUMO+2 have a Ge-F σ* character with the LUMO+1 being entirely based on the $OPMe_3$ ligand.

The HOMO, HOMO-1, and HOMO-2 of the geometric isomers of $[GeF_3(OPMe_3)_3]^+$ are also based on combinations of lone pairs on the F and O atoms. For these complexes the LUMO is mostly Ge-F antibonding and LUMO+1/+2 are mostly ligand-based. For both isomers of $[GeF_2(OPMe_3)_4]^{2+}$ the HOMO and HOMO-1/-2 are based on the lone pairs of the O and F atoms with the LUMO being mostly Ge-F antibonding and the LUMO+1/+2 mostly ligand-based (Figure 7 and SI).

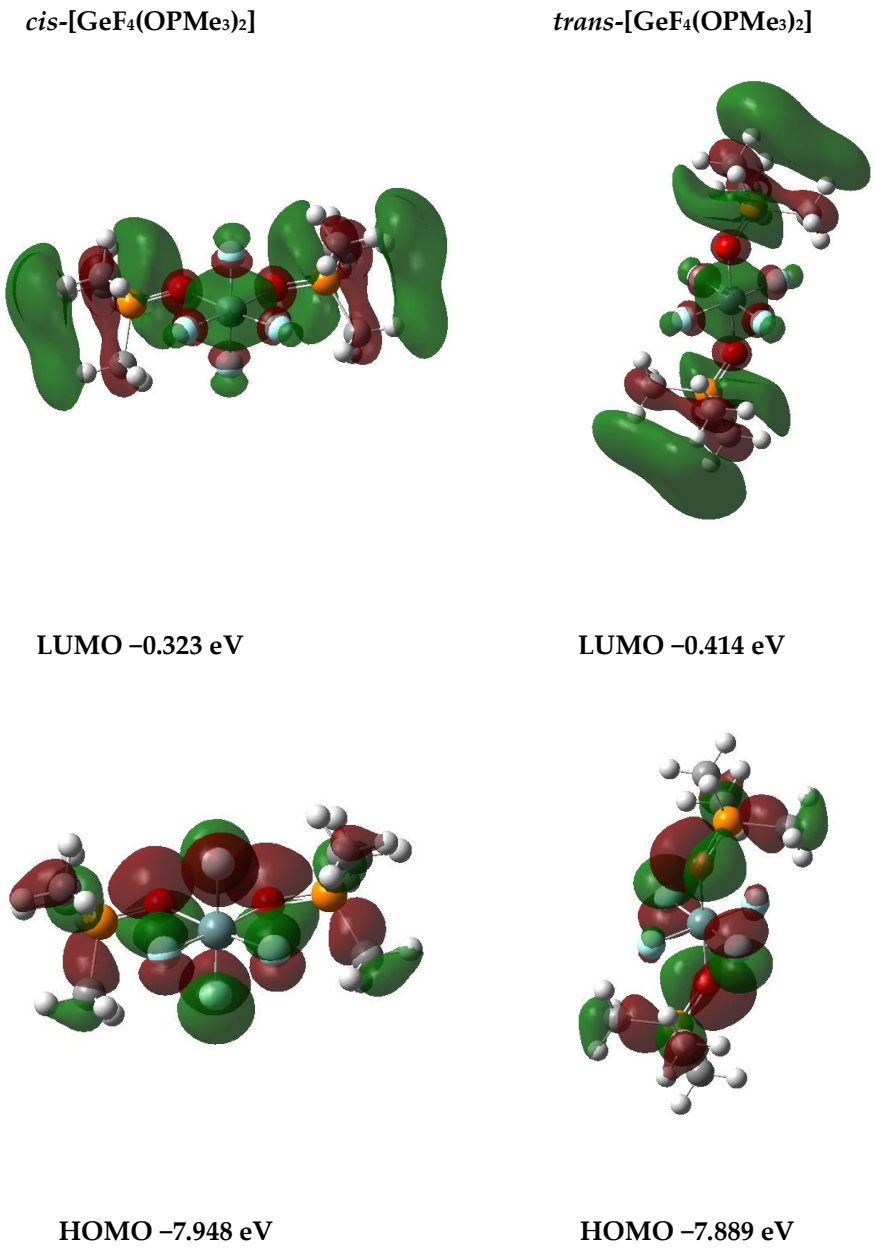

Figure 7. Representations of the HOMO and LUMO of *cis*- and *trans*-$[GeF_4(OPMe_3)_2]$.

3. Materials and Methods

The syntheses were carried out using standard Schlenk and vacuum line techniques, with samples handled and stored in a glove box under a dry dinitrogen atmosphere.

TMSOTf was obtained from Sigma-Aldrich and distilled before use. Germanium tetrafluoride was obtained from Fluorochem and used as received. CH_2Cl_2 and MeCN were dried by distillation from CaH_2 and n-hexane from sodium wire. Neutral ligands were obtained from Sigma-Aldrich unless otherwise stated and dried in vacuo (solids) or over molecular sieve (liquids) before use. Tacn (1,4,7-triazacyclononane) was prepared by the literature method [28] and the methylated versions, Me_3-tacn, Me_4-cyclen and Me_4-cyclam, were prepared from the parent macrocycles using the Eschweiler–Clarke reaction [29]. The germanium (IV) fluoride complexes, $[GeF_4(MeCN)_2]$, $[GeF_4(py)_2]$, $[GeF_4(OPPh_3)_2]$, $[GeF_4(OPMe_3)_2]$ and $[GeF_4(OAsPh_3)_2]$, were made by following the literature methods [13,14].

Infrared spectra were recorded as Nujol mulls between CsI plates using a PerkinElmer Spectrum 100 spectrometer over the range 4000–200 cm^{-1}. The ^1H $^{19}F\{^1H\}$ and $^{31}P\{^1H\}$ NMR spectra were recorded from CH_3NO_2/CD_3NO_2 or CH_2Cl_2/CD_2Cl_2 solutions unless otherwise stated, using a Bruker AV400 spectrometer and are referenced to Me_4Si (*via* the residual solvent resonance), $CFCl_3$, and 85% H_3PO_4, respectively. ESI^+ mass spectra were obtained in MeCN solution using a Waters Acquity Platform. Microanalyses were undertaken by Medac.

3.1. X-ray Experimental

Crystals of *mer*-$[GeF_3(OPPh_3)_3][OTf]$ and *cis*-$[GeF_2(Me_4\text{-cyclen})][OTf]_2$ xCH_3NO_2 were grown from CH_2Cl_2 solution and CH_3NO_2 solution, respectively. Data collection used a Rigaku AFC12 goniometer equipped with an enhanced sensitivity (HG) Saturn724+ detector mounted at the window of an FR-E+ SuperBright molybdenum (λ = 0.71073 Å) rotating anode generator with VHF Varimax optics (70 μm focus) with the crystal held at 100 K. Structure solution and refinement were performed using SHELX(S/L)97, SHELX-2013, or SHELX-2014/7.41 and OLEX [30–32]. H atoms bonded to C were placed in calculated positions using the default C–H distance and refined using a riding model. Analysis of the data for $[GeF_2(Me_4\text{-cyclen})][OTf]_2$ xCH_3NO_2 revealed an inversion twin with a surprisingly large unit cell in space group $P2_1$, with the asymmetric unit containing 14 cations, 28 anions and four CH_3NO_2 solvent molecules that were resolved, and a further 5.5 CH_3NO_2 solvent molecules per asymmetric unit were accounted for by solvent masking. There appeared to be no plausible higher symmetry space group and no missed symmetry. While the $[GeF_2(Me_4\text{-cyclen})]^{2+}$ cations were generally well-defined, some of the OTf groups showed evidence of some rotational disorder, most of which were modelled satisfactorily. Given the very large cell and the inversion twin, while the identity of the complex and the *cis* octahedral coordination geometry at Ge are not in doubt, detailed comparisons of the geometric parameters are not justified. Details of the crystallographic parameters are given in Table S1. CCDC reference numbers for the crystallographic information files in cif format are 2174295 ($[GeF_3(OPPh_3)_3][OTf]$) and 2177877 ($[GeF_2(Me_4\text{-cyclen})][OTf]_2$ xCH_3NO_2).

3.2. DFT Calculations

The electronic structures of the series $[GeF_4(OPMe_3)_2]$, $[GeF_3(OPMe_3)_3]^+$ and $[GeF_2(OPMe_3)_4]^{2+}$ were investigated by density functional theory (DFT) calculations using the Gaussian 16W program [33] and visualised using GaussView 5.0. The density functional chosen was B3LYP-D3 [34] with the basis set as 6-311G(d) [35]. Energy minima were confirmed by the absence of imaginary frequencies.

3.3. Complex Syntheses

$[GeF_4(dmso)_2]$: GeF_4 was gently bubbled through a stirred solution of dmso (1 mL) in n-hexane for 2 min. The solution was then stirred for 1 h at room temperature. The resulting white solid was filtered off and dried in vacuo. Yield 0.43 g. $C_4H_{12}F_4GeO_2S_2$(304.88): calcd. C 15.76, H 3.97; found C 15.91, H 3.31%. ^1H NMR (400 MHz, CD_3NO_2, 298 K): δ = 2.90 (br s, CH_3); (253 K): δ = 3.03 (br s, CH_3), 2.91 (s, CH_3). $^{19}F\{^1H\}$ NMR (CD_3NO_2, 298 K): δ = −112.5 (br), −112.8 (s), −128.2 (br); (253 K): δ = −115.3 (t, $^2J_{FF}$ = 61 Hz), −115.4 (s),

−129.8 (t, $^2J_{FF}$ = 61 Hz). IR (Nujol): $\tilde{\nu}$ = 944 (s), 914 (s) (S-O), 632 (br), 618 (br), 596 (br) (Ge-F) cm^{-1}.

[GeF_4(dmf)$_2$]: [GeF_4(MeCN)$_2$] (0.50 g, 2.2 mmol) was suspended in excess dmf and left to stir for 2 h at 50 °C, leading to a white precipitate forming. The solid was collected by filtration, washed with n-hexane (3 × 2 mL) and dried in vacuo. Yield 0.125 g, 60%. $C_6H_{14}F_4GeN_2O_2$ (294.81): calcd. C 24.44, H 4.79, N 9.50; found C 24.04, H 5.39. N 9.32%. ^{1}H NMR (400 MHz, CD_3NO_2, 298 K): δ = 8.19 (br m, H), 8.12 (br m, H), 3.29 (s, CH_3), 3.21 (s, CH_3), 3.13 (s, CH_3), 3.04 (s, CH_3); (253 K): δ = 8.16 (s, H), 8.13 (s, H), 3.28 (s, CH_3), 3.25 (s, CH_3), 3.12 (s, CH_3), 3.07 (s, CH_3). ^{19}F{^{1}H} NMR (CD_3NO_2, 298 K): δ = −124.8 (br), −125.5 (s), −136.6 (br); (253 K): δ = −125.4 (t, $^2J_{FF}$ = 59 Hz), −125.4 (s), −135.8 (t, $^2J_{FF}$ = 59 Hz). IR (Nujol): $\tilde{\nu}$ = 1678 (s), 1654 (s) (C = O), 642 (br), 622 (br), 587 (s) (Ge-F) cm^{-1}.

[GeF_4(pyNO)$_2$]: [GeF_4(MeCN)$_2$] (0.264 g, 1.14 mmol) was dissolved in CH_2Cl_2 and pyNO (0.517 g, 2.28 mmol) was added to the solution and left to stir for 2 h, forming a white precipitate. The solid was filtered off, washed in n-hexane (3 × 2 mL) and dried in vacuo. Yield 0.320 g, 41%. $C_{10}H_{10}F_4GeN_2O_2$ CH_2Cl_2 (423.8): calcd. C 31.18, H 2.85, N 6.61; found C 31.95, H 3.31, N 7.28%. ^{1}H NMR (400 MHz, CD_3NO_2, 298 K): δ = 8.7 (m, [2H]), 8.4 (m), 8.0 (m); (253 K): δ = 8.77 (m), 8.37 (m), 7.98 (m). ^{19}F{^{1}H} NMR (CD_3NO_2, 298 K): δ = −142.8 (br, s); (253 K): δ = −129.2(s), −132.3 (t, $^2J_{FF}$ = 58 Hz), −138.13 (t, $^2J_{FF}$ = 58 Hz). IR (Nujol): $\tilde{\nu}$ = 1206 (br) (N-O), 679 (s), 605 (s) (Ge-F) cm^{-1}.

[GeF_3(pyNO)$_3$][OTf]: TMSOTf (0.024 g, 0.11 mmol) was added to a solution of [GeF_4(pyNO)$_2$] (0.037 g, 0.11 mmol) in CH_2Cl_2 (10 mL) at room temperature. After stirring for 2 h, pyNO (0.095 g, 0.11 mmol) in MeCN (1 mL) was added. The reaction mixture was stirred for 72 h. The resulting white precipitate was filtered off, washed in n-hexane (15 mL) and dried in vacuo. Yield 0.54 g, 77%. $C_{16}H_{15}F_6GeN_3O_6S$ CH_2Cl_2 (648.9): calcd. C, 31.46, H 2.64, N 6.48; found C 31.62, H, 2.94, N, 7.18%. ^{1}H NMR (400 MHz, CD_3NO_2, 298 K): δ = 8.7 (m), 8.3 (m), 7.9 (m). ^{19}F{^{1}H} NMR (CD_3NO_2, 298 K): δ = −79.6 (s), −136.9 (d, $^2J_{FF}$ = 65 Hz), −141.8 (s), −143.0 (t, $^2J_{FF}$ = 65 Hz). IR (Nujol): $\tilde{\nu}$ = 639 (s), 590 (w) (Ge-F) cm^{-1}.

[GeF_3(dmso)$_3$][OTf]: TMSOTf (0.051 g, 0.23 mmol) was added to a solution of [GeF_4(dmso)$_2$] (0.070 g, 0.23 mmol) in CH_2Cl_2 (10 mL) at room temperature. After stirring for 2 h, dmso (0.23 mmol) in MeCN (1 mL) was added, and the reaction mixture was stirred for 72 h. The solvent was concentrated to ca. 5 mL, n-hexane (15 mL) was added, and the white solid produced was filtered and dried in vacuo. Yield 0.082 g, 69%. $C_7H_{18}F_6GeO_6S_4$ $2H_2O$ (549.1): calcd. C 15.03, H 4.04; found C 14.84, H 3.69%. ^{1}H NMR (400 MHz, CD_3NO_2, 298 K): δ = 3.06 (s, CH_3), 2.99 (s, CH_3), 2.98 (s, CH_3), 2.00 (s, H_2O). ^{19}F{^{1}H} NMR (CD_3NO_2, 298 K): δ = −79.1 (s), −109.8 (d, $^2J_{FF}$ = 71 Hz), −121.7 (t, $^2J_{FF}$ = 71 Hz), −122.2 (s). IR (Nujol): $\tilde{\nu}$ = 3437 (br) 1651 (m) (H_2O), 932 (m), 920 (m) (S-O), 639 (s), 590 (w) (Ge-F) cm^{-1}.

[GeF_3(dmf)$_3$][OTf]: TMSOTf (0.128 g, 0.50 mmol) was added to a solution of [GeF_4(dmf)$_2$] (0.170 g, 0.50 mmol) in CH_2Cl_2 (10 mL) at room temperature. After stirring for 2 h, dmf (0.50 mmol) in MeCN (1 mL) was added, and the reaction mixture was stirred for 72 h. The solvent was concentrated to ca. 5 mL, n-hexane (15 mL) was added, and the white solid was collected by filtration and dried in vacuo. Yield 0.110 g, 38%. $C_{10}H_{21}F_6GeN_3O_6S$ $2.5CH_2Cl_2$ (710.29): calcd. C 21.14, H 3.69, N 5.92; found C 20.60, H 3.48, N 6.08%. ^{1}H NMR (400 MHz, CD_3NO_2, 298 K): δ = 8.36 (s, H), 8.22 (s, H), 5.44 (CH_2Cl_2), 3.30–3.42 (m, CH_3), 3.14–3.24 (m, CH_3). ^{19}F{^{1}H} NMR (CD_3NO_2, 253 K): δ = −79.1 (s), −126.1 (d, $^2J_{FF}$ = 64 Hz), −134.5 (s), −135.0 (t, $^2J_{FF}$ = 64 Hz). IR (Nujol): $\tilde{\nu}$ = 1658 (vbr) (C = O), 638 (s), 590 (m) (Ge-F) cm^{-1}.

[GeF_3($OPPh_3$)$_3$][OTf]: TMSOTf (0.046 g, 0.20 mmol) was added to a solution of [GeF_4($OPPh_3$)$_2$] (0.144 g, 0.20 mmol) in CH_2Cl_2 (10 mL) at room temperature. After stirring for 2 h, $OPPh_3$ (0.056 g, 0.20 mmol) was added, and the reaction mixture was stirred for 15 h. The solvent was concentrated to ca. 5 mL, n-hexane (15 mL) was added, and the solid was filtered off and dried in vacuo. Yield 0.150 g, 67%. $C_{55}H_{45}F_6GeO_6P_3S$ $1.5CH_2Cl_2$

(1240.9): calcd. C 54.68, H 3.90; found C 55.22 H 3.98%. ^{1}H NMR (400 MHz, CD_2Cl_2, 298 K): δ = 7.7–7.3 (m). ^{19}F{^{1}H} NMR (CD_2Cl_2, 298 K): δ = −79.0 (s), −89.0 (d, $^{2}J_{FF}$ = 76 Hz), −100.4 (t, $^{2}J_{FF}$ = 76 Hz), −100.9 (s). ^{31}P{^{1}H} NMR (CD_2Cl_2, 298 K): δ = 44.1 (s), 43.7 (s), 41.7 (s). IR (Nujol): $\tilde{\nu}$ = 1116 (s), 1049 (m) (P = O), 637 (s), 578 (m), (Ge-F) cm^{-1}.

[$GeF_3(OPMe_3)_3$][OTf]: TMSOTf (0.089 g, 0.40 mmol) was added to a solution of [$GeF_4(OPMe_3)_2$] (0.070 g, 0.40 mmol) in CH_2Cl_2 (10 mL) at room temperature. After stirring for 2 h, $OPMe_3$ (0.110 g, 0.40 mmol) was added, and the reaction mixture was stirred for 15 h. A white precipitate gradually formed, and this was collected by filtration, washed with n-hexane (10 mL) and dried in vacuo. Yield 0.160 g, 72%. $C_{10}H_{27}F_6GeO_6P_3S$ (554.92): calcd. C 21.64, H 4.90; found C 21.44, H 4.25%. ^{1}H NMR (400 MHz, CD_3NO_2, 298 K): δ = 1.90 (d, $^{2}J_{PH}$ = 14 Hz), 1.83 (d, $^{2}J_{PH}$ = 14 Hz), 1.82 (d, $^{2}J_{PH}$ = 14 Hz). ^{19}F{^{1}H} NMR (CD_3NO_2, 298 K): δ = −79.8 (s), −93.0 (s), −95.7 (d, $^{2}J_{FF}$ = 64), −106.6 (t, $^{2}J_{FF}$ = 64 Hz). ^{31}P{^{1}H} NMR (CD_3NO_2, 298 K): δ = 70.4 (s), 67.4 (m), 66.9 (m). IR (Nujol): $\tilde{\nu}$ = 1149 (s), 1078 (s) ν (P = O), 639 (s), 600 (w) ν (Ge-F) cm^{-1}.

[$GeF_3(py)_3$][OTf]: TMSOTf (0.095 g, 0.43 mmol) was added to a solution of [$GeF_4(py)_2$] (0.131 g, 0.43 mmol) in CH_2Cl_2 (10 mL) at room temperature. After stirring for 2 h, pyridine (0.03 g, 0.43 mmol) was added to the solution and the reaction mixture was stirred for 15 h. The solvent was concentrated to ca. 5 mL, *n*-hexane (15 mL) was added, and the solid was filtered off and dried in vacuo. Yield 0.10 g, 47%. $C_{16}H_{15}F_6GeN_3O_3S\ CH_2Cl_2$ (600.92): calcd. C 33.98, H 2.85, N 6.99; found C 33.96, H 2.87, N 7.21%. ^{1}H NMR (400 MHz, CD_2Cl_2, 298 K): δ = 8.93 (m), 8.76 (m), 8.70 (m), 8.20 (m), 7.91 (m), 7.82 (m), 7.73 (m), 7.73 (m). ^{19}F{^{1}H} NMR (CD_2Cl_2, 298 K): δ = −79.0 (s), −122.0 (t, $^{2}J_{FF}$ = 55 Hz), −137.3 (d, $^{2}J_{FF}$ = 55 Hz), −149.2 (s). IR (Nujol): $\tilde{\nu}$ = 627 (br), 615 (br) (Ge-F) cm^{-1}.

[$GeF_3(OAsPh_3)_3$)][OTf] and [$GeF_2(OAsPh_3)_4$)][OTf]$_2$: TMSOTf (0.089 g, 0.40 mmol) was added to a solution of $GeF_4(MeCN)_2$] (0.092 g, 0.40 mmol) in CH_2Cl_2 and the reaction mixture was allowed to stir for 2 h. To this, $OAsPh_3$ (0.32 g, 1.20 mmol) was then added, and the solution was stirred for 15 h, affording a white precipitate which was separated by filtration, washed in hexane and dried in vacuo. Yield 0.21 g. ^{1}H NMR (CD_3NO_2, 298 K): 7.3–7.9 (m). ^{19}F{^{1}H} NMR (CD_3NO_2, 298 K): δ = −89.9 (s), −89.5 (t, $^{2}J_{FF}$ = 66 Hz), −79.9 (s, OTf), −79.3 (d, $^{2}J_{FF}$ = 67 Hz), −65.1 (s), −59.1 (s). IR (Nujol): $\tilde{\nu}$ = 845 (sh) (As = O), 636 (Ge-F) cm^{-1}. Since the ^{19}F NMR spectrum showed that both complexes were present (see Results and Discussion), microanalytical data were not recorded.

[GeF_3(terpy)][OTf]: TMSOTf (0.115 g, 0.52 mmol) was added to a solution of [$GeF_4(MeCN)_2$] (0.119 g, 0.52 mmol) in CH_2Cl_2 (10 mL) at room temperature. After stirring for 2 h, terpy (0.120 g, 0.52 mmol) was added, and the reaction mixture was stirred for 15 h. A white solid precipitated, which was separated by filtration, washed with *n*-hexane (3 × 5 mL) and dried in vacuo. Yield 0.150 g. Despite attempts on different batches both before and after attempted recrystallisation, satisfactory elemental analyses for this compound could not be obtained, most likely due to the very poor solubility of the complex and co-precipitation of inorganic materials with the complex. However, the spectroscopic data are consistent with that expected for the formulation, *mer*-[GeF_3(terpy)][OTf]. ^{1}H NMR (400 MHz, CD_2Cl_2, 298 K): δ = 9.3 (m, [2H]), 8.9 (m, [2H]), 8.8 (m, [2H]), 8.7 (m, [H]), 8.6 (m, [2H]), 8.2 (m, [2H]). ^{19}F{^{1}H} NMR (CD_2Cl_2, 298 K): δ = −79.0 (s), −115.9 (d, $^{2}J_{FF}$ = 68 Hz, [2F]), −153.0 (t, 68 Hz, [F]). IR (Nujol): $\tilde{\nu}$ = 637 (br), 573 (s) (Ge-F) cm^{-1}.

[GeF_3(Me$_3$-tacn)][OTf]: TMSOTf (0.243 g, 1.1 mmol) was added to a solution of [$GeF_4(MeCN)_2$] (0.302 g, 1.1 mmol) in MeCN (10 mL) at room temperature and stirred for 2 h. Me$_3$-tacn (0.188 g, 0.46 mmol) was then added, and a white solid precipitated immediately. This was stirred further for 15 h and the solid was separated by filtration, recrystallised from CH_3NO_2/Et_2O and dried in vacuo. Yield 0.260 g, 53%. $C_{10}H_{21}F_6GeN_3O_3S\ H_2O$ (467.99): calcd. C 25.67, H 4.95, N 8.98; found C 25.81, H 4.96, N 8.79%. ^{1}H NMR (400 MHz, CD_3NO_2, 298 K): δ = 3.4 (m, [12H]), 3.0 (s, [9H]), 2.0 (s, H_2O). ^{19}F{^{1}H} NMR (CD_3NO_2, 298 K): δ = −78.7 (s,

OTf), −151.7 (s). IR (Nujol): ṽ = 640 (s), 606 (s) (Ge-F) cm^{-1}. LRMS (ESI^+, CH_3NO_2): *m/z* calculated for M^+ = 300.92, found: 300.09.

[GeF_2(Me_4**-cyclen)][OTf]$_2$**: TMSOTf (0.547 g, 2.46 mmol) was added to a solution of [$GeF_4(MeCN)_2$] (0.284 g, 1.23 mmol) in CH_2Cl_2 and allowed to stir for 2 h. A solution of Me_4-cyclen (0.281 g, 1.23 mmol) in MeCN was then added, and the reaction mixture was left to stir for 86 h. The resulting yellow precipitate was filtered, washed with *n*-hexane (3 × 5 mL) and dried under a flow of nitrogen. Yield 0.520 g, 63%. $C_{16}H_{28}F_8GeN_4O_6S_2$: Calc. for C, 26.39; H, 4.43; N, 8.79. Found: C, 25.98; H, 4.65; N, 8.59%. ^{1}H NMR (CD_3NO_2, 298 K): δ = 3.82–4.00 (m, CH_2, [8H]), 3.51–3.70 (m, CH_2, [8H]), 3.34 (s, CH_3, [6H]), 3.05 (s, CH_3, [6H]). $^{19}F\{^1H\}$ NMR (CD_3NO_2, 298 K): δ = −79.3 (s, OTf), −132.3 (s). IR (Nujol): ṽ = 639 (m), 574 (m) (Ge-F) cm^{-1}. LRMS (ESI^+, CH_3NO_2): *m/z* calculated for M^{2+} = 170.07, found: 170.07.

[GeF_2(Me_4**-cyclam)][OTf]$_2$:** TMSOTf (0.618 g, 2.78 mmol) was added to a solution of [$GeF_4(MeCN)_2$] (0.321 g, 1.4 mmol)) in CH_2Cl_2 and allowed to stir for 2 h. A solution of Me_4-cyclam (0.357 g, 1.4 mmol) in CH_2Cl_2 was then added, and the reaction mixture was left to stir for 72 h. The resulting red-orange precipitate was filtered, washed with hexane (3 × 5 mL) and dried under a flow of nitrogen. Yield 0.42 g, 45%. $C_{16}H_{32}F_8GeN_4O_6S_2$·MeCN: Calcd. for C, 30.61; H, 5.00; N, 9.92. Found: C, 31.09; H, 5.10; N, 9.24%. ^{1}H NMR (CD_3NO_2, 298 K): δ = 3.30–3.07 (br m, CH_2, [20H]), 3.26 (s, CH_3, [3H]), 2.70 (br s, CH_3, [9H]). $^{19}F\{^1H\}$ NMR (CD_3NO_2, 298 K): δ ppm = −79.3 (s, OTf), −136.8 (d, $^2J_{FF}$ = 38 Hz), −134.8 (d, $^2J_{FF}$ = 52 Hz), −132.7 (s), −132.2 (d, $^2J_{FF}$ = 38 Hz), −130.8 (d, $^2J_{FF}$ = 52 Hz), −130.5 (s). IR (Nujol): ṽ = 639 (s) (Ge-F) cm^{-1}. LRMS (ESI^+, CH_3NO_2): *m/z* calculated for M^{2+} = 184.09, found: 184.09.

4. Conclusions

A series of fluoro-germanium (IV) cations [GeF_3L_3][OTf] with neutral N- and O-donor co-ligands (L = dmso, dmf, pyNO, $OPPh_3$, $OPMe_3$, py) was prepared and fully characterised. In solution they exist as mixtures of *mer* and *fac* isomers, with the *mer* dominating. The attempts to prepare dications by removal of a further fluoride were only successful for L = $OAsPh_3$ (partially) and for the two tetra-aza macrocycles. The [GeF_3L_3][OTf] are similar to [SnF_3L_3][OTf] [21], but appear to be less stable in solution, and whilst mixtures of [SnF_3L_3][OTf] and [SnF_2L_4][OTf]$_2$ were formed by the reaction of [SnF_4L_2] or [SnF_3L_3][OTf] with TMSOTf and more L (although only [$SnF_2(OPPh_3)_4$][OTf]$_2$ was isolated in a pure form), the similar removal of a second fluoride in the germanium systems did not occur for most of the L investigated. Standard sources [36] suggest that Sn-F and Ge-F bonds differ little in energy (456 and 464 kJ/mol, respectively), and there may be a significant kinetic factor in the germanium case. Such a situation is much more common in transition-metal rather than main-group chemistry, where partially filled *d*-orbitals and significant interactions of the ligands with the transition-metal *d*-orbitals can give rise to very significant kinetic barriers. Notably, in the present study the tetra-aza macrocyclic complex syntheses, [GeF_2L''][OTf]$_2$, required some 3 days to go to completion. Further, the ability of $OAsPh_3$ to form [$GeF_2(OAsPh_3)_4$][OTf]$_2$ contrasts with OPR_3, suggesting that $OAsPh_3$ is a stronger donor towards the fluoro-germanium (IV) centre. This is consistent with crystallographic data on isostructural early transition-metal pnictine oxide complexes, which showed that the M-OAs bond length was shorter than that for M-OP, suggesting stronger binding of the $OAsPh_3$ towards hard acceptors.

The DFT calculations provided evidence for trends in the stability of the isomers, although it should be remembered that the calculations are for gas-phase ions, and cation/anion interactions, packing effects in the solids, and solvation in solution will significantly affect the stabilities.

Supplementary Materials: The following supporting information can be downloaded at: https://www.mdpi.com/article/10.3390/inorganics10080107/s1, spectroscopic data: Figure S1. [$GeF_4(dmso)_2$]; Figure S2. [$GeF_4(dmf)_2$]; Figure S3. [$GeF_4(pyNO)_2$]; Figure S4. [$GeF_3(dmso)_3$][OTf]; Figure S5.

$[GeF_3(dmf)_3][OTf]$; Figure S6. $[GeF_3(py)_3][OTf]$; Figure S7. $[GeF_3(pyNO)_3][OTf]$; Figure S8. $[GeF_3(OPPh_3)_3][OTf]$; Figure S9. $[GeF_3(OPMe_3)_3][OTf]$; Figure S10. $[GeF_3(OAsPh_3)_3][OTf]$ and $[GeF_2(OAsPh_3)_4][OTf]_2$; Figure S11. $[GeF_3(terpy)][OTf]$; Figure S12. $[GeF_3(Me_3\text{-tacn})][OTf]$; Figure S13. $[GeF_2(Me_4\text{-cyclen})][OTf]_2$; Figure S14. $[GeF_2(Me_4\text{-cyclam})][OTf]_2$; Table S1. X-ray crystallographic data; Figure S15. Frontier orbitals of *cis*/*trans*-$[GeF_4(OPMe_3)_2]$; Figure S16. Frontier orbitals of *fac*/*mer*-$[GeF_3(OPMe_3)_3]^+$; Figure S17. Frontier orbitals of *cis*/*trans*-$[GeF_2(OPMe_3)_4]^{2+}$. Table S2. The x,y,z coordinates used in the DFT calculations are also included.

Author Contributions: Conceptualization, W.L. and G.R.; Data curation, M.S.W. and R.P.K.; Formal analysis, M.S.W. and R.D.B.; Funding acquisition, G.R.; Investigation, M.S.W., R.P.K. and R.D.B.; Methodology, R.P.K., W.L. and G.R.; Resources, J.G. and G.M.; Supervision, W.L. and G.R.; Validation, R.D.B.; Writing—original draft, W.L.; Writing—review & editing, M.S.W., R.P.K., J.G., G.M. and G.R. All authors have read and agreed to the published version of the manuscript.

Funding: This research was funded by a CASE studentship to M.S.W from GE Healthcare and EPSRC grant number EP/R513325/1, and by EPSRC through grant numbers EP/N035437/1, EP/N509747/1 and through the EPSRC Mithras Programme Grant (EP/S032789/1).

Data Availability Statement: CCDC reference numbers for the crystallographic information files in cif format are 2174295 ($[GeF_3(OPPh_3)_3][OTf]$) and 2177877 ($[GeF_2(Me_4\text{-cyclen})][OTf]_2\ xCH_3NO_2$). These data can be obtained free of charge via http://www.ccdc.cam.ac.uk/conts/retrieving.html (accessed on 20 June 2022), or from the Cambridge Crystallographic Data Centre, 12 Union Road, Cambridge CB2 1EZ UK.

Acknowledgments: We thank J. M. Dyke for helpful discussions regarding the DFT calculations.

Conflicts of Interest: The authors declare no conflict of interest.

References

1. McCleverty, J.A.; Meyer, T.J. (Eds.) *Comprehensive Coordination Chemistry II*; Elsevier: Oxford, UK, 2004; Volume 3.
2. Downs, A.J. *Chemistry of Aluminium, Gallium, Indium and Thallium*; Blackie & Son Publishing: London, UK, 1993.
3. Smith, P.J. (Ed.) *The Chemistry of Tin*; Chapman & Hall: London, UK, 1998.
4. Levason, W.; Reid, G.; Zhang, W. Coordination complexes of silicon and germanium halides with neutral ligands. *Coord. Chem. Rev.* **2011**, *255*, 1319–1341. [CrossRef]
5. Constable, E.C.; Parkin, G.; Que, L., Jr. (Eds.) *Comprehensive Coordination Chemistry III*; Elsevier: Oxford, UK, 2021; Volume 3.
6. Benjamin, S.L.; Levason, W.; Reid, G. Medium and high oxidation state metal/non-metal fluoride and oxide–fluoride complexes with neutral donor ligands. *Chem. Soc. Rev.* **2013**, *42*, 1460–1499. [CrossRef] [PubMed]
7. Levason, W.; Monzittu, F.M.; Reid, G. Coordination chemistry and applications of medium/high oxidation state metal and non-metal fluoride and oxide-fluoride complexes with neutral donor ligands. *Coord. Chem. Rev.* **2019**, *391*, 90–130. [CrossRef]
8. Bhalla, R.; Darby, C.; Levason, W.; Luthra, S.K.; McRobbie, G.; Reid, G.; Sanderson, G.; Zhang, W. Triaza-macrocyclic complexes of aluminium, gallium and indium halides: Fast ^{18}F and ^{19}F incorporation via halide exchange under mild conditions in aqueous solution. *Chem. Sci.* **2014**, *5*, 381–391. [CrossRef]
9. Bhalla, R.; Levason, W.; Luthra, S.K.; McRobbie, G.; Monzittu, F.M.; Palmer, J.; Reid, G.; Sanderson, G.; Zhang, W. Hydrothermal synthesis of Group 13 metal trifluoride complexes with neutral N-donor ligands. *Dalton Trans.* **2015**, *44*, 9569–9580. [CrossRef]
10. Chansaenpak, K.; Vabre, B.; Gabbaï, F.P. [^{18}F]-Group 13 fluoride derivatives as radiotracers for positron emission tomography. *Chem. Soc. Rev.* **2016**, *45*, 954–971. [CrossRef]
11. Blower, P.J. A nuclear chocolate box: The periodic table of nuclear medicine. *Dalton Trans.* **2015**, *44*, 4819–4844. [CrossRef]
12. Tudela, D.; Rey, F. Reactions of tin (II) fluoride with halogens. *Z. Anorg. Allgem. Chem.* **1989**, *575*, 202–208. [CrossRef]
13. Cheng, F.; Davis, M.F.; Hector, A.L.; Levason, W.; Reid, G.; Webster, M.; Zhang, W. Synthesis, spectroscopic and structural systematics of complexes of germanium(IV) halides (GeX_4, X = F, Cl, Br or I) with phosphane oxides and related oxygen donor ligands. *Eur. J. Inorg. Chem.* **2007**, *2007*, 2488–2495. [CrossRef]
14. Cheng, F.; Davis, M.F.; Hector, A.L.; Levason, W.; Reid, G.; Webster, M.; Zhang, W. Synthesis, spectroscopic and structural systematics of complexes of germanium(IV) halides (GeX_4, X = F, Cl, Br or I) with mono-, bi- and tri-dentate and macrocyclic nitrogen donor ligands. *Eur. J. Inorg. Chem.* **2007**, *2007*, 4897–4905. [CrossRef]
15. Davis, M.F.; Levason, W.; Reid, G.; Webster, M. Complexes of germanium(IV) fluoride with phosphane ligands: Structural and spectroscopic authentication of germanium(IV) phosphane complexes. *Dalton Trans.* **2008**, *2008*, 2261–2269. [CrossRef] [PubMed]
16. King, R.P.; Levason, W.; Reid, G. Neutral and cationic germanium(iv) fluoride complexes with phosphine coordination—Synthesis, spectroscopy and structures. *Dalton Trans.* **2021**, *50*, 17751–17765. [CrossRef] [PubMed]
17. Davis, M.F.; Levason, W.; Reid, G.; Webster, M.; Zhang, W. The first examples of germanium tetrafluoride and tin tetrafluoride complexes with soft thioether coordination—Synthesis, properties and crystal structures. *Dalton Trans.* **2008**, *2008*, 533–538. [CrossRef]

18. Suter, R.; Swidan, A.; Macdonald, C.L.B.; Burford, N. Oxidation of a germanium(II) dication to access cationic germanium(IV) fluorides. *Chem. Commun.* **2018**, *54*, 4140–4143. [CrossRef]
19. MacDonald, E.; Doyle, L.; Chitnis, S.S.; Werner-Zwanziger, U.; Burford, N.; Decken, A. Me_3P complexes of p-block Lewis acids $SnCl_4$, $SnCl_3^+$ and $SnCl_2^2$. *Chem. Commun.* **2012**, *48*, 7922–7924. [CrossRef] [PubMed]
20. Greenacre, V.K.; Levason, W.; King, R.P.; Reid, G. Neutral and cationic phosphine and arsine complexes of tin (IV) halides: Synthesis, properties, structures and anion influence. *Dalton Trans.* **2019**, *48*, 17097–17105. [CrossRef]
21. King, R.P.; Woodward, M.S.; Grigg, J.; McRobbie, G.; Levason, W.; Reid, G. Tin (IV) fluoride complexes with neutral phosphine coordination and comparisons with hard N-and O-donor ligands. *Dalton Trans.* **2021**, *50*, 14400–14410. [CrossRef]
22. Everett, M.; Jolleys, A.; Levason, W.; Light, M.E.; Pugh, D.; Reid, G. Cationic aza-macrocyclic complexes of germanium (II) and silicon (IV). *Dalton Trans.* **2015**, *44*, 20898–20905. [CrossRef]
23. Waller, A.W.; Weiss, N.M.; Decato, D.A.; Phillips, J.A. Structural and energetic properties of haloacetonitrile–GeF_4 complexes. *J. Mol. Struct.* **2017**, *1130*, 984–993. [CrossRef]
24. Levason, W.; Patel, B.; Popham, M.C.; Reid, G.; Webster, M. Scandium, yttrium and lanthanum nitrate complexes of tertiary arsine oxides: Synthesis and multinuclear spectroscopic studies. X-ray structures of $[M(Me_3AsO)_6](NO_3)_3$ (M = Sc or Y), $[Sc(Ph_3AsO)_3(NO_3)_2]NO_3$, $[M''(Ph_3AsO)_4(NO_3)_2]NO_3$ (M'' = Y or La) and $[La(Ph_3AsO)_2(EtOH)(NO_3)_3]$. *Polyhedron* **2001**, *20*, 2711–2720.
25. Jura, M.; Levason, W.; Petts, E.; Reid, G.; Webster, M.; Zhang, W. Taking TiF_4 complexes to extremes-the first examples with phosphine co-ligands. *Dalton Trans.* **2010**, *39*, 10264–10271. [CrossRef] [PubMed]
26. Benjamin, S.L.; Levason, W.; Pugh, D.; Reid, G.; Zhang, W. Preparation and structures of coordination complexes of the very hard Lewis acids ZrF_4 and HfF_4. *Dalton Trans.* **2012**, *41*, 12548–12557. [CrossRef] [PubMed]
27. Griffiths, J.E.; Irish, D.E. Vibrational spectrum of the hexafluorogermanate ion. *Inorg. Chem.* **1964**, *3*, 1134–1137. [CrossRef]
28. Wieghardt, K.; Chaudhuri, P.; Nuber, B.; Weiss, J. New triply hydroxo-bridged complexes of chromium(III), cobalt(III), and rhodium(III): Crystal structure of tris(.mu.-hydroxo)bis[(1,4,7-trimethyl-1,4,7-triazacyclononane)chromium(III)] triiodide trihydrate. *Inorg. Chem.* **1982**, *21*, 3086–3090. [CrossRef]
29. Barefield, E.K.; Wagner, F. Metal complexes of 1, 4, 8, 11-tetramethyl-1, 4, 8, 11-tetraazacyclotetradecane, N-tetramethylcyclam. *Inorg. Chem.* **1973**, *12*, 2435–2439. [CrossRef]
30. Sheldrick, G.M. Crystal structure refinement with SHELXL. *Acta Crystallogr. Sect. C Struct. Chem.* **2015**, *71*, 3–8. [CrossRef]
31. Sheldrick, G.M. A short history of SHELX. *Acta Crystallogr. Sect. A Found. Crystallogr.* **2008**, *64*, 112–122. [CrossRef]
32. Dolomanov, O.V.; Bourhis, L.J.; Gildea, R.J.; Howard, J.A.K.; Puschmann, H.J. Synthesis and Structure of Ferrocenol Esters. *Appl. Crystallogr.* **2009**, *42*, 339–341. [CrossRef]
33. Frisch, M.J.; Trucks, G.W.; Schlegel, H.B.; Scuseria, G.E.; Robb, M.A.; Cheeseman, J.R.; Scalmani, G.; Barone, V.; Petersson, G.A.; Nakatsuji, H.; et al. *Gaussian 16W, Revision C.01*; Gaussian, Inc.: Wallingford, CT, USA, 2016.
34. Lee, C.; Yang, W.; Parr, R.G. Development of the Colle-Salvetti correlation-energy formula into a functional of the electron density. *Phys. Rev. B* **1988**, *37*, 785–789. [CrossRef]
35. Krishnan, R.; Binkley, J.S.; Seeger, R.; Pople, J.A. Self-consistent molecular orbital methods. XX. A basis set for correlated wave functions. *J. Chem. Phys.* **1980**, *72*, 650–654. [CrossRef]
36. Yu, Y.-R. *Comprehensive Handbook of Chemical Bond Energies*; CRC Press: Boca Raton, FL, USA, 2007.